

Published in final edited form as:

Traffic. 2009 December ; 10(12): 1773–1784. doi:10.1111/j.1600-0854.2009.00992.x.

Roles of an Unconventional Protein Kinase and Myosin II in Amoeba Osmotic Shock Responses

Venkaiah Betapudi and Thomas T. Egelhoff*

Department of Cell Biology, Cleveland Clinic Foundation, 9500 Euclid Avenue, Cleveland, OH 44195

Abstract

The contractile vacuole (CV) is a dynamic organelle that enables *Dictyostelium* amoeba and other protist to maintain osmotic homeostasis by expelling excess water. In the present study, we have uncovered a mechanism that coordinates the mechanics of the CV with myosin II, regulated by VwkA, an unconventional protein kinase that is conserved in an array of protozoa. GFP-VwkA fusion proteins localize persistently to the CV during both filling and expulsion phases of water. In *vwkA* null cells, the established CV marker *dajumin* still localizes to the CV, but these structures are large, spherical, and severely impaired for discharge. Furthermore, myosin II cortical localization and assembly are abnormal in *vwkA* null cells. Parallel analysis of wild type cells treated with myosin II inhibitors or of myosin II null cells also results in enlarged CVs with impaired dynamics. We suggest that the myosin II cortical cytoskeleton, regulated by VwkA, serves a critical conserved role in the periodic contractions of the CV, as part of the osmotic protective mechanism of protozoa.

Keywords

Dictyostelium; alpha kinases; myosin II; osmotic shock; contractile vacuoles

Introduction

The contractile vacuole (CV) is a contractile osmoregulatory organelle found in *Dictyostelium*, *Paramecium*, *Trypanosomes*, and other protozoa (1;2). The CV functions as a “bladder”, activated particularly in settings of hypoosmotic stress, where it rhythmically enlarges, filling with liquid, then fuses transiently with the plasma membrane in conjunction with rapid collapse, expelling the liquid contents to the extracellular environment. As noted by Allen (3), the dramatic contractile behavior of this organelle was recorded among the earliest studies performed by the first microscopists in the 1700s (4). In the best studied systems such as *Dictyostelium* and *Paramecium*, the vacuole is connected to a subcellular tubular network hypothesized to be part of the water delivery/accumulation system of the cell. Protein-translocating ATPases, calmodulin, and an array of possible regulatory proteins have been localized to this structure in *Dictyostelium* and *Paramecium* (3;5–7). Aquaporin water channels have also been localized to the CV in amoeba proteus, in *Leshmania*, and in *Trypanosomes* (2;8;9). Despite a wealth of studies on this organelle, the mechanisms by which it regulates ion fluxes and water accumulation remain poorly understood.

*Address for all correspondence: Dr. Thomas T. Egelhoff, Department of Cell Biology (NC10), The Lerner Research Institute, Cleveland Clinic Foundation, 9500 Euclid Avenue, Cleveland, OH 44195, USA, Tel (216) 445-9912, Fax (216) 444-9404, egelhot@ccf.org.

Live cell imaging studies have revealed a series of marker proteins that associate with the CV, such as dajumin, persistently associated with the CV (10), and LvsA, which associates transiently during the expulsion step (11). Localization of Rab11A, Rab14, and RabGAP-domain proteins such as drainin have strongly implicated GTPase cycles as having roles in CV function as well (12). The recent characterization of disgorgin, a Rab8A-GAP, established an elegant regulatory pathway critical in governing the normal mechanics of CV growth, plasma membrane fusion, and expulsion phases (6). Together with earlier studies, this work established a model in which Rab11A, Rab11C, and dajumin are associated with the CV tubular network at an early stage in the cycle. With enlargement and filling, drainin, disgorgin, and Rab8A are recruited to the CV membrane. Late in the cycle LvsA is recruited, fusion and discharge occur, and the cycle reinitiates.

Despite the accumulating understanding of what players associate with the CV and participate in the regulation of the cycle, remarkably little is understood about the mechanics of the cycle, and regarding what forces drive the dramatic motile contractility of the organelle. Localization of myosin I to CVs in multiple systems (7;13) led to suggestions that motors might either help move CVs to proximity with the plasma membrane, or that myosin-based contraction might directly drive the dramatic constriction event. More recent EM studies have revealed a striking paucity of any actin filaments on the surface of the CV, arguing against a direct acto-myosin contraction occurring on the surface of the organelle (1). Another class of models for CV contraction driving force proposes membrane curvature-inducing proteins as a source of tension to drive the expulsion/contraction step. This concept has been proposed in *Paramecium* (14). In *Dictyostelium*, the BEACH domain protein LvsA is recruited to the CV concurrent with the contraction/collapse phase. Given the similarity of LvsA to mammalian proteins that can induce membrane curvature, it has been proposed that LvsA might help drive contraction via inducing membrane curvature/tension in the CV (11;15). F-BAR proteins similarly can induce membrane curvature, and *Dictyostelium* members of this family also localize to the CV and associated tubule system and participate in CV function (16). Whether such membrane curvature inducing proteins directly affect contraction, or perhaps participate in creating/maintaining the associated tubule system, remains unresolved.

In earlier work we reported the localization of an unconventional protein kinase, VwkA, to the CV system in *Dictyostelium*. VwkA is a member of a family of “alpha” kinases in this amoeba (17). The other characterized members of this family are all established myosin II heavy chain kinases (MHCK A, MHCK B, and MHCK C). VwkA was notable compared to the other characterized members of the family, in that while catalytically active *in vitro* for autophosphorylation and for phosphorylation of the *in vitro* substrate myelin basic protein, the kinase showed only weak activity towards myosin II. While the direct physiological substrate for VwkA remains unclear, we demonstrate here that VwkA has an important role in contractile vacuole dynamics and in hypo-osmotic shock survival. VwkA null cells display excessive numbers of engorged CVs which fail to undergo proper fusion with the plasma membrane. We further show that these cells have aberrant cortical myosin II organization, and that perturbation of myosin II abundance or activity also results in defective CV dynamics. These studies argue for a role for myosin II based cytosolic tension in CV contractile function, and for a role for VwkA in the regulation of these events.

Results

VwkA is the founding example of a highly conserved group of protein kinases found in many protozoa

VwkA displays a distinctive domain organization, with an amino-terminal von Willebrand Factor A (vWFA) domain, as well as the carboxyl-terminal alpha kinase domain. The vWFA

domains are a structural motif found in an array of proteins, thought to mediate protein-protein interactions in diverse functions ranging from transcription, DNA repair, ribosomal and membrane transport, to proteosomal functions (18). At the time of the initial characterization of Vwka (17), NCBI genomic databases revealed only one other protein kinase gene displaying a related domain architecture, from *Neurospora crassa*. With the completion of more genome projects, however, it is now clear that Vwka displays a domain architecture that is highly conserved in multiple lower eukaryotes (Figure 1). An evaluation of current entries in the Conserved Domain Architecture Retrieval Tool (CDART) at the National Center for Biotechnology Information (NCBI) reveals a striking array of domain-organization homologues of Vwka, present in the genomes of a number of protozoa, including *Tetrahymena*, *Paramecium*, *Chlamydomonas*, as well as in *Neurospora*, and diatoms of the genus *Thalassiosira*. All of these proteins contain conserved amino-terminal vWFA domains adjacent to carboxyl-terminal alpha kinase domains. We suggest that this strong conservation of domain architecture reflects a conserved role for Vwka and its protist homologues in osmoregulation and CV function.

Multiple domains in Vwka contribute to localization to the CV

To gain insights in the mechanism of Vwka localization to the CV, parental *Dictyostelium* Ax2 cells expressing GFP-conjugated sub-fragments of Vwka were generated using plasmid constructs that express either the vWFA domain (GFP-vWFA) or the catalytic domain (GFP-CAT; Figure 2A & B). Intracellular localization studies of these constructs were performed via parallel imaging of GFP and FM2-10, a lipophilic styryl fluorescent dye that preferentially labels the CV in live cells (5;19). As with the full-length kinase fusion (GFP-Vwka), both subdomains GFP constructs localize robustly to the CV (Figure 2C). Although a catalytically “kinase dead” construct (GFP-KD) still localized to the CV, expression of this construct in parental Ax2 cells resulted in enlarged CVs that showed reduced contractility, suggesting a dominant negative effect on CV function. These results indicate that at least two independent structural signals can localize Vwka to the CV, with one signal in the vWFA domain and one in the catalytic domain

Vwka⁻ and Vwka⁺⁺ cells display impaired cell shape recovery and reduced viability following osmotic shock

The CV system in *Dictyostelium* or other protist consists of interconnected tubules that control the water balance inside the cell by accumulating and expelling excess water from the cytoplasm (3;5;12). During the execution of this protective mechanism cells undergo shape changes by inducing the rearrangement of their cortex proteins (20–22). Our previous studies suggested a Vwka role in the regulation of the cytoskeletal protein myosin II (17). We therefore examined whether cellular shape changes or morphological responses to osmotic shock might be altered in vwkA⁻ cells and Vwka-hyperexpressing cells (Vwka⁺⁺; generated by passing cells in high G418 selection to increase plasmid copy number (17)). Cells were allowed to attach to cover slip chambers in HL5 medium overnight, and then imaged before and after replacement of the medium with water. As with the parental Ax2 cells, both vwkA⁻ and Vwka⁺⁺ cells round up rapidly upon the initial osmotic shock (Figure 3). Parental Ax2 cells re-spread and resume relatively normal morphology by 30 min. On the other hand, Vwka⁻ and Vwka⁺⁺ cells remained rounded up for at least 30 min post-shock. This behavior is reminiscent to the morphological defects observed in cells lacking the endogenous expression of the BEACH protein LvsA and AP-1 Clathrin-adaptor proteins that are known to bind the CV system in *Dictyostelium* (11;23;24). These results suggest that Vwka⁻ and Vwka⁺⁺ cells are osmosensitive and Vwka has role in regulating the CV responses to hypo-osmotic challenges.

As a further test of possible roles of VwkA and of myosin II in hypo-osmotic shock responses, we monitored cell death following incubation of cells in water for 1 hour. Flow cytometry analysis revealed an increase in cell death in both *vwkA* cells and myosin II null cells, relative to parental cells, in response to osmotic shock (Figure 4). This behavior further suggests possible roles for VwkA and myosin II in cell survival responses following hypo-osmotic shock.

VwkA⁻ cells have abnormal CV in hypotonic conditions

To understand VwkA roles in the regulation of the CV, time lapse imaging was performed of the cells in HL5 growth medium and water, and compared to AP180⁻ cells previously described as having abnormal CV behavior in hypo-osmotic conditions (25). This analysis revealed presence of ~2–3 contractile vacuoles/cell, undergoing periodic contractions and expansions (Figure 5A). There was no significant difference in the average number of CV present in the wild type Ax2 versus VwkA⁻ or VwkA⁺⁺ cells growing in HL5 medium (Figure 5B). However, the abundance of CVs increased throughout the cytoplasm when the HL5 growth medium is replaced with water (Figure 5B). The average number of CV per cell under hypotonic conditions was more than doubled as compared to cells growing in HL5 medium. Increase in the diameter of CV occurred both in the parental Ax2 and the VwkA⁻ cells, but the enlargement of CV was significantly higher in cells lacking VwkA (Figure 5A, arrow-heads, and Figure 5C). These enlarged CVs are reminiscent of the CV observed in osmosensitive AP180 null cells described earlier (25).

The periodic contraction and expansion of CVs was monitored via time lapse imaging for several minutes. CVs in parental AX2 cells displayed a repeated expansion/collapse cycles. However, the CVs present in VwkA⁻ and AP180⁻ cells frequently remained large without undergoing contractions for several minutes. We compared the maximum enlargement of CV that occurs in the wild type Ax2 and VwkA⁻ cells by using time-lapse DIC images of the cells in water. The maximum diameter of each CV was recorded in the cells challenged to hypo-osmotic conditions. This analysis showed a significant increase in the average maximum diameter of CVs present in VwkA⁻ and AP180⁻ cells (Figure 5C). In most cases the enlarged CV never underwent a fusion/collapse transition during the course of video analysis. These severely impaired CV dynamics suggest that VwkA has a critical role in the regulation of CV function during osmotic stress responses.

Impaired CV dynamics in VwkA⁻ cells

To understand VwkA roles in regulating the dynamics of CV, we performed time-lapse imaging of the live cells incubated in water with FM2-10 dye. Parental Ax2 cells displayed FM2-10-labeled CVs undergoing rhythmic expansion and collapse, with an average lifetime of ~150 sec (Figure 6A & C). We measured the diameter of each CV as well the life time of each CV, from first appearance until plasma membrane fusion/collapse. A typical AX2 time lapse movie reveals many CV fusion/collapse events within 3–5 minutes. Parallel analysis of *vwkA* null cells revealed a larger average size for CVs (Figure 6A & B), and dramatically longer CV lifetime (Figure 6C). Due to a near-complete absence of any detectable fusion/collapse events in short duration (3–5 min) time-lapse movies, image acquisition was extended out to the 10–15 minute range in an attempt to capture full CV cycles. Even with the longer duration imaging, many identified CVs failed to undergo fusion/collapse during the imaging period. To confirm these results, we generated cells expressing dajumin-GFP, a marker for the CV (10). As shown in Figure 6D, dajumin-GFP localizes to CV in both Ax2 and VwkA⁻ cells. The CV in VwkA⁻ cells are nearly circular in comparison with more irregular CV structures in Ax2 cells. The dajumin-GFP labeled CVs in *vwkA* null cells were larger than CVs present in Ax2 cells (Figure 6E), and again, in *vwkA* null cells these structures were frequently static for the duration of video analysis, rarely displaying a

contraction or collapse phase even with extended 10–15 min imaging periods (Figure 6F). These results established that markers such as dajumin still localize to the CVs in *vwkA* null cells, but that the CVs are nonetheless defective in the contraction/collapse phase of the normal cycle.

Myosin II is necessary for normal CV function

Earlier studies have demonstrated that myosin II phosphorylation accompanies high-glucose hyper-osmotic shock responses (20), but cellular hyper-osmotic shock responses are not known to involve the CV in any way. To our knowledge there have been no studies addressing whether myosin II has roles in the regulation of morphology and dynamics of CV functions. Given our earlier studies indicating that *VwkA* gene disruption had an effect on myosin II expression and assembly levels, we investigated whether pharmacological inhibition of myosin II, or myosin II gene disruption, would alter CV morphology or dynamics. Treatment of parental Ax2 cells with the myosin II motor activity inhibitor blebbistatin (26) in HL5 medium resulted in a significant increase in average maximum CV diameter assessed from video analysis (Figure 7A). Average maximum CV size upon blebbistatin treatment was similar to the average maximum size observed for myosin II null cells in HL5 medium, supporting the argument that myosin II contractile activity contributes to normal CV cycling. When myosin II nulls cells were placed in water, their average maximum CV diameter was not affected by blebbistatin treatment (Figure 7B), confirming that myosin II is the target being affected by this inhibitor in this assay. Further analysis of CV behavior in the absence of myosin II was performed by transfecting myosin II null cells with the dajumin-GFP marker. As in the *vwkA* null cells, dajumin-GFP was able to localize to the CV, but dynamics were impaired, with large and non-contractile CVs observed in many cells (Figure 7C).

Myosin II organization is abnormal in *vwkA* null cells during osmotic shock recovery

Previous work revealed an increase in abundance and overassembly of endogenous myosin II in *vwkA* null cells (17). The current work reveals a similar increase in abundance when a plasmid-based GFP-myosin II construct is expressed in *vwkA* null cells (with expression driven from a constitutive actin 15 promoter; Figure 8A & B). This result suggests that elevated myosin II abundance in *vwkA* null cells is a post-transcriptional effect. In addition to the modest increase in GFP-myosin II abundance in *vwkA* null cells, we observed abnormal cortical organization for GFP-myosin II when expressed in *vwkA* null cells following transfer from HL5 growth medium into water. GFP-myosin II was observed to translocate and accumulate in the cell cortex following osmotic shock in both parental Ax2 and in the *vwkA* null background (Figure 8C). In the *vwkA* null background myosin II displayed a clumped and irregular organization, particularly after the osmotic challenge. These results suggest that myosin II dynamics, and proper control of the abundance and organization of cortical myosin II, are impaired in the absence of the *VwkA* protein. Abnormal cortical organization in the *vwkA* null background included clumps of GFP-myosin II (Figure C), reminiscent of aggregates observed in earlier studies when myosin II overassembly was forced via disruption of the established MHC II kinases MHCK A, B, and C (27). These results extend our earlier work showing a slight overassembly of myosin II in *vwkA* null cells (17), and strongly suggest that *VwkA* somehow helps control cytoskeletal organization during osmotic shock responses.

Discussion

VwkA was first identified in *Dictyostelium* via genomic database approaches, as one of six unconventional “alpha kinases” in this organism (17). The founding three members of this group had been demonstrated at the biochemical and cellular level to function as myosin II

heavy chain kinases (MHCKs) controlling myosin II filament assembly, and were denoted MHCK A, B, and C (28–30). These enzymes carried a signature carboxyl-terminal WD-repeat domain that was shown to mediate kinase targeting to myosin II filaments (31). Our initial biochemical and cellular characterization of VwkA revealed a very different domain organization from the previously characterized MHCKs, with no WD-repeat domain, but rather with an amino-terminal von Willebrand factor A (vWFA) motif. Our biochemical studies (17) demonstrated VwkA to have robust autophosphorylation activity, and robust ability to phosphorylate general protein kinase substrates such as myelin basic protein, but when incubated with Mg-ATP and Dictyostelium myosin II, purified VwkA displayed no detectable ability to phosphorylate this substrate. However, it was also observed that the purified VwkA bound strongly to calmodulin in the presence of calcium, and in this setting we observed weak but detectable phosphorylation of myosin II heavy chains. These results left matters equivocal as to whether myosin II was a bone fide physiological substrate for VwkA. Our current *in vivo* studies suggest that despite weak VwkA kinase activity towards myosin II *in vitro*, the possibility that VwkA may be a contractile vacuole-restrict MHC II kinase merits further consideration.

Our current observation that VwkA localizes strongly to the CV, and that *vwkA* null cells display severe defects in contractile vacuole fusion/discharge has led us to further examination of possible roles of this enzyme in CV function. Although myosin II reorganization has been implicated in responses to high glucose levels and associated hyperosmotic shock (20), to our knowledge there are no previous reports implicating myosin II in CV function or CV dynamics. In fact, deep-etch EM analysis by Heuser has established the absence of any significant actin cytoskeleton on CV membranes (1), making the concept of direct acto-myosin contraction of the CV unlikely. However, our current observations suggest that myosin II does play roles in CV biology.

We suggest that myosin II affects contractile vacuole dynamics on at least two levels, as outlined in the model in Figure 9. First, impaired CV behavior in myosin II null cells, or upon myosin II inhibition with blebbistatin, indicate a positive role for myosin II in fusion of the CV to the plasma membrane, and/or the contractile expulsion phase. Earlier studies have argued for cytosolic pressure as a driving force for the expulsion/contraction phase of the CV cycle (3). We propose that cortical myosin II, via its baseline contractile activity, contributes to cytosolic pressure, and that this pressure helps drive CV collapse when the mature CV fuses with the plasma membrane.

Secondly, we suggest that the cortical shell of actomyosin also functions as a barrier that can inhibit the fusion of the mature CV with the plasma membrane. A strong positive role for the type V myosin *myoJ* was recently reported for osmoregulation and for cortical associate of the CV to the plasma membrane (32). Those studies support the idea that a cortical F-actin barrier may exist, with which the CV membrane must associate prior to fusion with the plasma membrane.

A strong parallel exists between this step of the normal CV life cycle and the analogous phase of synaptic vesicle fusion. As discussed by Heuser (1), in both cases a “kiss and run” mechanism appears to be used, where the lipid bilayer of the vesicle or vacuole fuses with the plasma membrane and releases internal contents. However, in both cases the lipids of the vesicle or vacuole do not appear to mix with or disperse into the plasma membrane bilayer. Rather, the vesicle membrane, after briefly docking and fusing with the plasma membrane, appears to undock and be re-internalized (1;33). In the chromaffin cell setting, a cortical barrier of F-actin inhibits fusion of resting chromaffin vesicles with the plasma membrane (34). Recent studies have further demonstrated a role for myosin II in fusion pore expansion (35). This behavior is strikingly similar to the behavior of the CV in Dictyostelium. Earlier

work demonstrated that pharmacological reduction of F-actin content biases CV fusion to a more complete collapse state (1), and the current studies, described in this work indicate a role for VwkA in the fusion of the CV to the plasma membrane. We suggest that VwkA facilitates the removal of a cytoskeletal barrier at the final stages of the CV life cycle, allowing the fusion machinery of the two membranes to engage. VwkA may act indirectly, or it may in fact function as a MHCK in this setting to help disassemble the cortical cytoskeleton. In the latter scenario, we suggest that high levels of calmodulin on the CV membrane (7) could be part of the mechanism activating VwkA to disassemble myosin II filaments. Although calcium/calmodulin potently activated VwkA in our earlier biochemical work, the activity of the enzyme towards myosin II in those biochemical studies was modest (17). We suggest that some additional unidentified CV-restricted factor existing may trigger full activity of VwkA towards myosin II. Finally, given the strong conservation of the VwkA domain architecture among many lower eukaryotes, we suggest that the role served by VwkA is likely conserved in CV function among many species.

A likely positive role for myosin II in driving CV collapse and expulsion does not rule out a role for alternative models that have been proposed. Strong lines of evidence support the model that membrane curvature-inducing proteins contribute to formation and maintenance of the tubular ductal collecting system of the protist osmoregulatory system, and these tension-inducing proteins might contribute to driving the fusion/expulsion events as well (15;16).

Materials and Methods

Strains and cell growth

We used the laboratory wild-type strain AX2 for generating *vwkA*⁻ cells and to generate cells expressing GFP fusions of VwkA, dajumin (10) and myosin II (36). We grew cells as described earlier (17). Note that two different types of FLAG-VwkA expressing cell lines were used in this work. “VwkA⁺⁺” refers to cells passaged repeatedly in G418 at 50 µg/ml to select for strong overexpression (used for some morphological studies in this work. “VwkA-rescued” refers to FLAG-VwkA cell lines selected and passaged in G418 at 8 µg/ml. Myosin II nulls used throughout this work are the *mhcA* null cell line “HS1” that has been described previously (37).

Cloning

GFP-vWFA was created by cloning PCR product of vWFA domain using primer P1 (5'-GTCGAGCTCGCAATTAGAGCATCGGAGTGTGTTG-3') and P2 (5'-CGATCTAGAGCAAGGGGCATCAGCGATATGAATTAC-3') in pTX-GFP plasmid vector (38). PCR product of catalytic domain amplified by using P3 (5'-GCAGGATCCATGTTACAAACAAAATTTAAAATGCCATC-3') and P4 (5'-TGTTCTAGATTAATAAGAATATGAAATAGAAGAGGAAGATG-3') primers was cloned in pTX-GFP to create GFP-Cat. Double PCR fusion product generated with primers P5 (5'-CGATGTAGCATCAAACAGATG-3'), C592A_{low} (5'-CCTAATTTTTTAGCATGCATATTACATTTATG-3'), C592A_{top} (5'-CATAAATGTAATATGCATGCTAAAAAATTAGG-3') and P6 (5'-CGATCTAGATTAATAAGAATATGAAATAGAAGAGG-3') was cloned into pTX-GFP to generate GFP-KD.

Western blot analysis

Preparation of total cell lysates and western blot analysis were performed as described earlier (17). All SDS-PAGE was performed with 4–20% commercial gradient gels (Invitrogen).

Microscopy methods

DIC and GFP imaging of the cells were performed by using Zeiss 510 confocal microscope. Cells were washed with PDF buffer pH 6.7 (1.32 mM KH_2PO_4 , 1.10 mM K_2HPO_4 , 2 mM KCl, 0.10 mM CaCl_2 , and 0.25 mM MgSO_4) before adding water to study CV dynamics. CV dynamics by using FM2-10 dye was performed as described earlier (17). For time lapse analysis of CV dynamics, movies were generated with a 100X n.a. 1.4 oil objective, and a 488 nm laser was used to illuminate the GFP. Laser power was always kept at or below 2% power to reduce any phototoxicity. For fluorescent imaging of FM2-10 or for imaging of GFP, movie frames were collected at 10 sec or 20 sec intervals, with a total duration never more than 15 min to avoid phototoxicity. For DIC transmitted light movies, frames were collected at 20 sec intervals, but longer duration imaging is possible. Acquisition details for each movie are provided here: movie 1 (10 sec interval, 30 frames, 5 min duration); movie 2 (20 sec interval, 20 frames, 6.7 min duration), movie 3 (20 sec interval, 20 frames, 6.7 min duration), movie 4 (10 sec interval, 80 frames, 13 min duration), movie 5 (10 sec interval, 60 frames, 10 min duration), movie 6 (10 sec interval, 60 frames, 10 min duration), and movie 7 (10 sec interval, 60 frames, 10 min duration).

Data analysis

In all figures box and whisker plots were generated with standard Sigma Plot settings, and display the median value flanked by two grey boxes that indicate 2nd and 3rd quartiles of the data set. Whiskers indicate the boundaries for the 10th and 90th percentile of each data set range. Dots represent the 5th and 95th percentiles of the data set.

Cell death assay by flow cytometry

Cell death assay using propidium iodide staining was performed as described earlier (39) with some modifications. Ten million cells growing in plastic plates in HL5 medium were collected by centrifugation at room temperature. After rinsing with phosphate buffered saline (PBS), cells were incubated in 500 μl of either PBS or distilled water at room temperature for 60 min. Propidium iodide solution was added to a final concentration of 4 μM and then cells were subjected to flow cytometry analysis light scatter and fluorescent readout.

Supplementary Material

Refer to Web version on PubMed Central for supplementary material.

Acknowledgments

This work was supported by NIH grant GM50009 to T.T.E.

References

1. Heuser J. Evidence for recycling of contractile vacuole membrane during osmoregulation in *Dictyostelium amoebae*--a tribute to Gunther Gerisch. *Eur J Cell Biol.* 2006; 85:859–71. [PubMed: 16831485]
2. Rohloff P, Docampo R. A contractile vacuole complex is involved in osmoregulation in *Trypanosoma cruzi*. *Exp Parasitol.* 2008; 118:17–24. [PubMed: 17574552]
3. Allen RD. The contractile vacuole and its membrane dynamics. *Bioessays.* 2000; 22:1035–42. [PubMed: 11056480]
4. Spallanzani, L. *Opuscoli di fisica animale e vegetabile.* Modena: Societa Tipografica; 1776.
5. Gerisch G, Heuser J, Clarke M. Tubular-vesicular transformation in the contractile vacuole system of *Dictyostelium*. *Cell Biol Int.* 2002; 26:845–52. [PubMed: 12421575]

6. Du F, Edwards K, Shen Z, Sun B, De LA, Briggs S, et al. Regulation of contractile vacuole formation and activity in *Dictyostelium*. *EMBO J*. 2008; 27:2064–76. [PubMed: 18636095]
7. Zhu Q, Clarke M. Association of calmodulin and an unconventional myosin with the contractile vacuole complex of *Dictyostelium discoideum*. *J Cell Biol*. 1992; 118:347–58. [PubMed: 1629238]
8. Nishihara E, Yokota E, Tazaki A, Orii H, Katsuhara M, Kataoka K, et al. Presence of aquaporin and V-ATPase on the contractile vacuole of *Amoeba proteus*. *Biol Cell*. 2008; 100:179–88. [PubMed: 18004980]
9. Figarella K, Uzcategui NL, Zhou Y, LeFurgey A, Ouellette M, Bhattacharjee H, et al. Biochemical characterization of *Leishmania major* aquaglyceroporin LmAQP1: possible role in volume regulation and osmotaxis. *Mol Microbiol*. 2007; 65:1006–17. [PubMed: 17640270]
10. Gabriel D, Hacker U, Kohler J, Muller-Taubenberger A, Schwartz JM, Westphal M, et al. The contractile vacuole network of *Dictyostelium* as a distinct organelle: its dynamics visualized by a GFP marker protein. *J Cell Sci*. 1999; 112 (Pt 22):3995–4005. [PubMed: 10547360]
11. Gerald NJ, Siano M, De Lozanne A. The *Dictyostelium* LvsA protein is localized on the contractile vacuole and is required for osmoregulation. *Traffic*. 2002; 3:50–60. [PubMed: 11872142]
12. Becker M, Matzner M, Gerisch G. Drainin required for membrane fusion of the contractile vacuole in *Dictyostelium* is the prototype of a protein family also represented in man. *EMBO J*. 1999; 18:3305–16. [PubMed: 10369671]
13. Doberstein SK, Baines IC, Wiegand G, Korn ED, Pollard TD. Inhibition of contractile vacuole function in vivo by antibodies against myosin-I. *Nature*. 1993; 365:841–3. [PubMed: 8413668]
14. Tani T, Allen RD, Naitoh Y. Cellular membranes that undergo cyclic changes in tension: Direct measurement of force generation by an in vitro contractile vacuole of *Paramecium multimicronucleatum*. *J Cell Sci*. 2001; 114:785–95. [PubMed: 11171384]
15. De Lozanne A. The role of BEACH proteins in *Dictyostelium*. *Traffic*. 2003; 4:6–12. [PubMed: 12535270]
16. Heath RJ, Insall RH. *Dictyostelium* MEGAPs: F-BAR domain proteins that regulate motility and membrane tubulation in contractile vacuoles. *J Cell Sci*. 2008; 121:1054–64. [PubMed: 18334553]
17. Betapudi V, Mason C, Licate L, Egelhoff TT. Identification and Characterization of a Novel α -Kinase with a von Willebrand Factor A-like Motif Localized to the Contractile Vacuole and Golgi Complex in *Dictyostelium discoideum*. *Mol Biol Cell*. 2005; 16:2248–62. [PubMed: 15728726]
18. Whittaker CA, Hynes RO. Distribution and evolution of von Willebrand/integrin A domains: widely dispersed domains with roles in cell adhesion and elsewhere. *Mol Biol Cell*. 2002; 13:3369–87. [PubMed: 12388743]
19. Heuser J, Zhu Q, Clarke M. Proton pumps populate the contractile vacuoles of *Dictyostelium amoebae*. *J Cell Biol*. 1993; 121:1311–27. [PubMed: 8509452]
20. Kuwayama H, Ecke M, Gerisch G, Van Haastert PJ. Protection against osmotic stress by cGMP-mediated myosin phosphorylation. *Science*. 1996; 271:207–9. [PubMed: 8539621]
21. Aizawa H, Katadae M, Maruya M, Sameshima M, Murakami-Murofushi K, Yahara I. Hyperosmotic stress-induced reorganization of actin bundles in *Dictyostelium* cells over-expressing cofilin. *Genes Cells*. 1999; 4:311–24. [PubMed: 10421841]
22. Zischka H, Oehme F, Pintsch T, Ott A, Keller H, Kellermann J, et al. Rearrangement of cortex proteins constitutes an osmoprotective mechanism in *Dictyostelium*. *EMBO J*. 1999; 18:4241–9. [PubMed: 10428962]
23. Wang J, Virta VC, Riddelle-Spencer K, O'Halloran TJ. Compromise of clathrin function and membrane association by clathrin light chain deletion. *Traffic*. 2003; 4:891–901. [PubMed: 14617352]
24. Lefkir Y, de Chassey B, Dubois A, Bogdanovic A, Brady RJ, Destaing O, et al. The AP-1 clathrin adaptor is required for lysosomal enzymes sorting and biogenesis of the contractile vacuole complex in *Dictyostelium* cells. *Mol Biol Cell*. 2003; 14:1835–51. [PubMed: 12802059]
25. Stavrou I, O'Halloran TJ. The monomeric clathrin assembly protein, AP180, regulates contractile vacuole size in *Dictyostelium discoideum*. *Mol Biol Cell*. 2006; 17:5381–9. [PubMed: 17050736]
26. Straight AF, Cheung A, Limouze J, Chen I, Westwood NJ, Sellers JR, et al. Dissecting temporal and spatial control of cytokinesis with a myosin II Inhibitor. *Science*. 2003; 299:1743–7. [PubMed: 12637748]

27. Yumura S, Yoshida M, Betapudi V, Licate LS, Iwadata Y, Nagasaki A, et al. Multiple Myosin II Heavy Chain Kinases: Roles in Filament Assembly Control and Proper Cytokinesis in *Dictyostelium*. *Mol Biol Cell*. 2005; 16:4256–66. [PubMed: 15987738]
28. Futey LM, Medley QG, Cote GP, Egelhoff TT. Structural analysis of myosin heavy chain kinase A from *Dictyostelium*. Evidence for a highly divergent protein kinase domain, an amino-terminal coiled-coil domain, and a domain homologous to the β -subunit of heterotrimeric G proteins. *J Biol Chem*. 1995; 270:523–9. [PubMed: 7822274]
29. Clancy CE, Mendoza MG, Naismith TV, Kolman MF, Egelhoff TT. Identification of a Protein Kinase from *Dictyostelium* with Homology to the Novel Catalytic Domain of Myosin Heavy Chain Kinase A. *J Biol Chem*. 1997; 272:11812–5. [PubMed: 9115238]
30. Liang W, Licate L, Warrick H, Spudich J, Egelhoff T. Differential localization in cells of myosin II heavy chain kinases during cytokinesis and polarized migration. *BMC Cell Biol*. 2002; 3:19. [PubMed: 12139770]
31. Steimle PA, Naismith T, Licate L, Egelhoff TT. WD Repeat Domains Target *Dictyostelium* Myosin Heavy Chain Kinases by Binding Directly to Myosin Filaments. *J Biol Chem*. 2001; 276:6853–60. [PubMed: 11106661]
32. Jung G, Titus MA, Hammer JA III. The *Dictyostelium* type V myosin MyoJ is responsible for the cortical association and motility of contractile vacuole membranes. *J Cell Biol*. 2009; 186:555–70. [PubMed: 19687255]
33. Harata NC, Aravanis AM, Tsien RW. Kiss-and-run and full-collapse fusion as modes of exo-endocytosis in neurosecretion. *J Neurochem*. 2006; 97:1546–70. [PubMed: 16805768]
34. Vitale ML, Seward EP, Trifaro JM. Chromaffin cell cortical actin network dynamics control the size of the release-ready vesicle pool and the initial rate of exocytosis. *Neuron*. 1995; 14:353–63. [PubMed: 7857644]
35. Doreian BW, Fulop TG, Smith CB. Myosin II activation and actin reorganization regulate the mode of quantal exocytosis in mouse adrenal chromaffin cells. *J Neurosci*. 2008; 28:4470–8. [PubMed: 18434525]
36. Moores SL, Sabry JH, Spudich JA. Myosin dynamics in live *Dictyostelium* cells. *Proc Natl Acad Sci USA*. 1996; 93:443–6. [PubMed: 8552657]
37. Ruppel KM, Uyeda TQ, Spudich JA. Role of highly conserved lysine 130 of myosin motor domain. In vivo and in vitro characterization of site specifically mutated myosin. *J Biol Chem*. 1994; 269:18773–80. [PubMed: 8034630]
38. Levi S, Polyakov M, Egelhoff TT. Green Fluorescent Protein and Epitope Tag Fusion Vectors for *Dictyostelium discoideum*. *Plasmid*. 2000; 44:231–8. [PubMed: 11078649]
39. Kosta A, Laporte C, Lam D, Tresse E, Luciani MF, Golstein P. How to assess and study cell death in *Dictyostelium discoideum*. *Methods Mol Biol*. 2006; 346:535–50. [PubMed: 16957313]

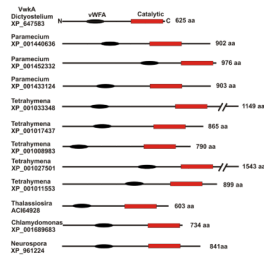


Figure 1. Conserved architecture of Vwka relatives throughout the protist phyla
 Examples identified with the NCBI CDART (Conserved Domain Architecture Retrieval Tool). The conserved vWFA domain (black oval) is a presumed scaffolding or protein/protein interaction motif. The conserved “alpha kinase” catalytic domain is shown as a red rectangle.

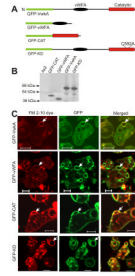


Figure 2. Redundant signals in VwkA drive localization to the contractile vacuole
 (A) Schematic organization of GFP-VwkA constructs. (B) Western blot confirming construct expression in Ax2 cells (C) FM2-10 staining demonstrates that both the vWFA domain (GFP-vWFA) and the catalytic domain (GFP-CAT) can drive the localization of VwkA constructs to the contractile vacuole. Kinase activity is not necessary for localization to the CV (GFP-KD). Scale bars, 5 μ m. Arrows indicate colocalization of the FM2-10 dye and each of the GFP fusion constructs. Also see movie 1, GFP-VwkA CV dynamics in parental Ax2 cells.

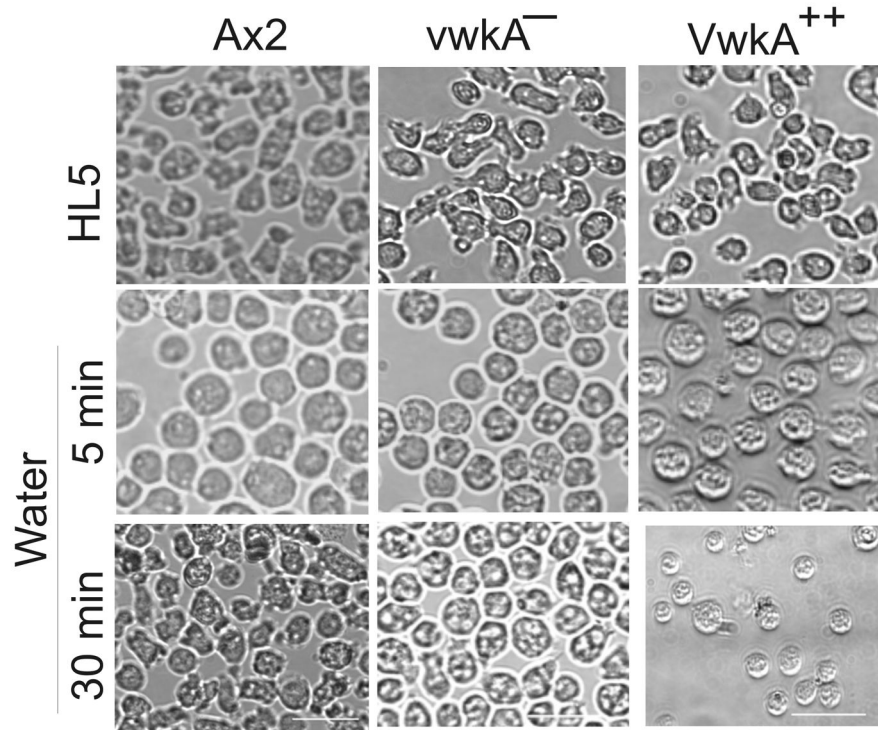


Figure 3. Vwka⁻ and Vwk hyper-expressing cells (Vwka⁺⁺) display impaired cell morphology response following hypo-osmotic shock

Parental Ax2, vwkA⁻, and Vwka⁺⁺ cells were collected in HL5 growth medium and seeded on glass bottom chambered dishes to 80–90% confluence. After one hour, images of the cells were recorded (top row). Cells were then subjected to osmotic shock by replacing growth medium with water. Images of the cells were collected again after 5 min (middle row) and 30 min (bottom row). The vwkA⁻ and Vwka⁺⁺ cells fail to respread efficiently after the initial rounding up response upon osmotic shock. Scale bar, 10 μ M.

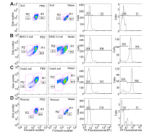


Figure 4. VwKA protects cells from cell death induced by hypo-osmotic shock

Indicated cell types, attached to plastic petri dishes, were switched from HL5 medium to either PBS or water for 60 minutes, then collected for viability analysis based up flow cytometry-based light scattering properties and propidium iodide (PI) staining, using recently described methods (39). Identified based on light scattering properties, the R1 population represents healthy cells and the R2 population is enriched in dying cells. The left two columns indicate the water-induced increase in the R2 population observed in mhA^- cells (**B**) and $vwkA^-$ cells (**C**), which is not observed in either parental Ax2 (**A**) nor in $vwkA^-$ cells rescued with a full-length plasmid-based VwKA cDNA (**D**). The right two column report PI staining for each water-treated set of cells, scored either in the R1 population (third column from left) or in the R2 population (last column on right). This PI analysis reveals a strong increase in PI-staining dead cells in the mhA^- population (**B**), and in the $vwkA^-$ population (**C**), which is not observed in either parental Ax2 (**A**) nor in $vwkA^-$ cells rescued with a full-length plasmid-based VwKA cDNA (**D**).

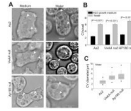


Figure 5. Vwka⁻ cells show abnormal contractile vacuoles in water

(A) Vwka⁻ cells display enlarged contractile vacuoles in water. Cells were seeded in glass bottom chambers to 70–80% confluence in HL5 medium, and video images collected starting after 1 hour (left panels). Parallel samples had medium replaced with water at 1 hour after plating (right panels), and video frames were analyzed after another 10–20 min. Arrowheads indicate contractile vacuoles. (B) CVs increase in number in all cell lines in response to hypo osmotic shock. CVs were counted in each cell line in media, or 10–20 min after replacing medium with water. Bars represent S.E. values. For all three cell lines, number of CVs in media were similar, and the number of CVs in all three lines increased significantly in water (n=50–60). (C) The diameter of contractile vacuoles in vwkA null and AP180 null cells in water are significantly larger than those of Ax2 cells. The average CV diameter for the two knockout lines differ statistically from the parental Ax2 (P=<0.001; n=34–54.) Box and whisker plot method details are described in Materials and Methods. Scale bars, 5 μM.

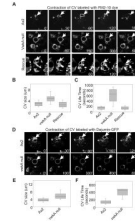


Figure 6. Impaired contractile vacuole dynamics in *vwka*⁻ cells

Cells were seeded in glass bottom chambers to 70–80% confluence in HL5 medium. After removing growth medium cells were rinsed with PDF buffer twice, then water with FM2-10 dye was added. Confocal images were collected at either 10 sec or 20 sec interval, see Materials and Methods for details. (A). FM2-10-labeled CVs displaying expansion and contraction when Ax2 cells are placed in water, while *vwka* null cells display impaired dynamics. Transfection (rescue) with FLAG-VwKA restores CV dynamics. See movie 2, CV dynamics in *vwka* null cells; movie 3, CV dynamics in VwKA rescued cells. (B) Quantitation of defects upon *vwka* gene disruption. Diameter of each FM2-10-stained CV was measured, from video frames, at its maximum size during the duration of the video analysis. Values of *vwka* null samples are statistically different from parental Ax2 ($P < 0.001$; $n = 38–54$). The average maximum CV size in the rescued cell line was statistically indistinguishable from the Ax2 line. Box and whisker plots as in figure 3. (C) CV lifetime is greatly prolonged in *vwka* null cells. CV lifetime was measured starting with frame 1 of movie, or from first appearance of any given CV, and measured to the last frame or to the frame in which CV displayed discharge/collapse. Average CV lifetime of *vwka* null cells was statistically different from Ax2 ($P < 0.001$; $n = 38–54$). Note that for quantitation, any CV that persisted for the full duration of the image series was scored as having a life time equal to the duration of the movie (800 sec for the quantitation analysis). Since Ax2 CVs never persisted for 800 sec, but *vwka* CVs frequently persisted for 800 sec, the quantitative analysis presented in this figure under-represent the true difference between parental and mutant cells. (D) CV dynamics monitored with the CV marker dajumin-GFP, in water. (E) Dajumin-GFP labeled *vwka* null cells display enlarged contractile vacuoles. (F) CV lifetime in *vwka* null cells scored by dajumin-GFP signal. In panels E and F, values of *vwka* null samples are statistically different from Ax2 ($P < 0.001$; $n = 26–29$). Scale bar, 5 μM .

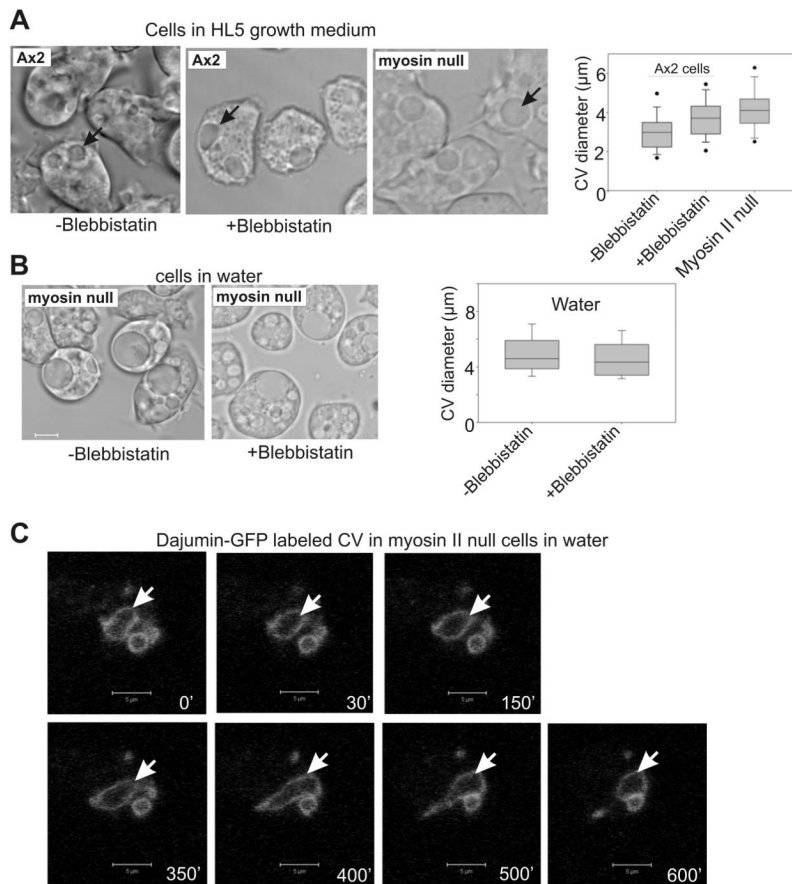


Figure 7. Myosin II is necessary for normal contractile vacuole function

(A) Parental Ax2 cells display enlarged CVs in the presence of blebbistatin. Myosin II null cells also display enlarged CV diameters in HL5 medium. Box and whisker graph quantifies average maximal CV diameters, determined from video analysis. Average maximum CV size for Ax2 cells in blebbistatin, and myosin II null cells, both differ from the untreated Ax2, $P < 0.02$, ($n = 53-54$). (B) Myosin II null cells display larger maximum CVs in water than do parental Ax2 cells, and size is not affected by the myosin II inhibitor blebbistatin. (C) Myosin II null cells expressing CV marker protein dajumin-GFP display impaired CV dynamics. Cells were imaged after transferring cells from HL5 medium to water. Arrow denotes a persistent contractile vacuole. Scale Bars, 5 μm . See movie 4, CV dynamics of parental Ax2 cells in water, no blebbistatin; movie 5, CV dynamics of Ax2 cells in water, with blebbistatin; movie 6, CV dynamics of myosin II null cells in water, no blebbistatin; movie 7, CV dynamics of myosin null cells in water, with blebbistatin.

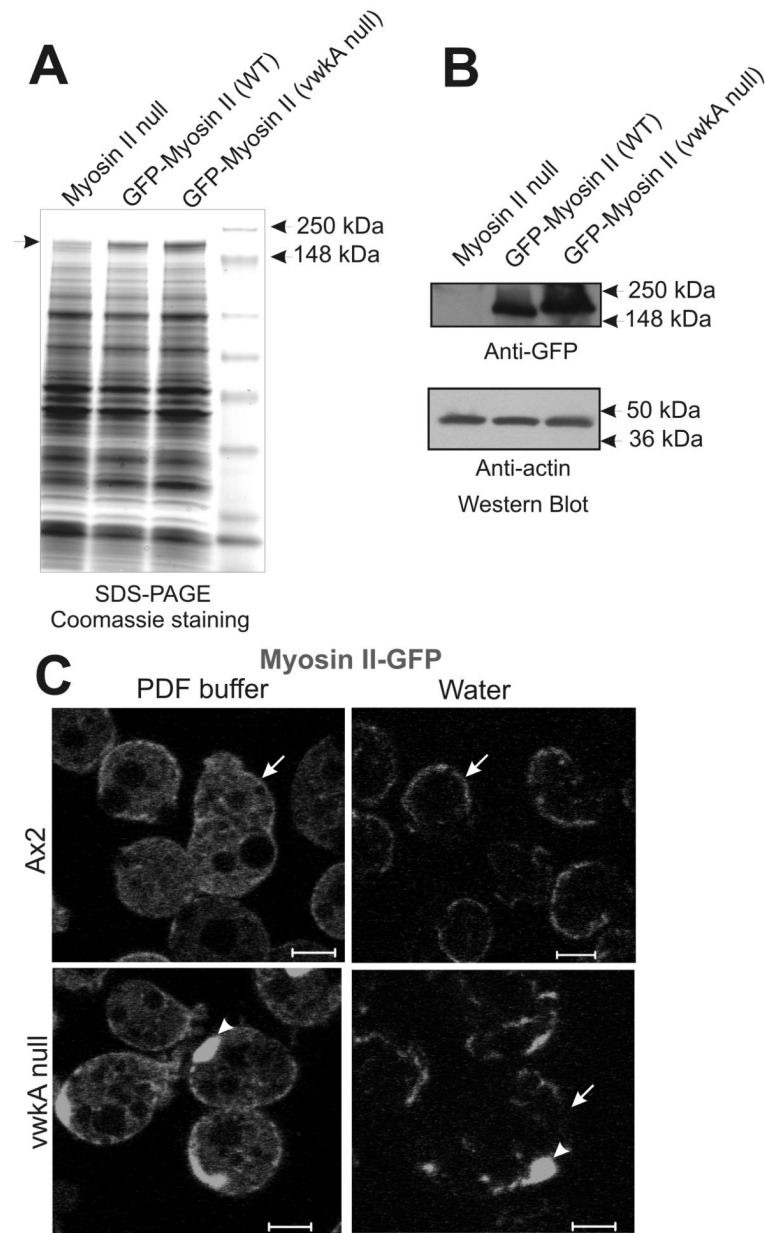


Figure 8. Impaired localization of GFP -myosin II to cell membrane in vwKA null cells
 (A) SDS-polyacrylamide gel reveals Coomassie-detectable elevated abundance of GFP-myosin when construct is expressed in vwKA null background, relative to the level when the same construct is expressed in the parental background. Arrow denotes position of the GFP-myosin II. (B) Anti-GFP western blot documenting elevated expression of GFP-myosin II when expressed in vwKA null background. Lower portion of western blot was probed for actin as a loading control. Signal quantitation via densitometry reports a 2.5-fold increase in signal for the GFP-myosin II level in the vwKA null background relative to the level of this protein when expressed in the parental Ax2 background. (C) When transfected into the vwKA null background, GFP-myosin II displays irregular clumped appearance before and after a 5' osmotic shock. Arrowheads indicate cortical clumps of GFP-myosin II, arrows emphasize the more irregular organization of GFP-myosin II in the vwKA null background after osmotic shock. Scale bars, 5 μ M.

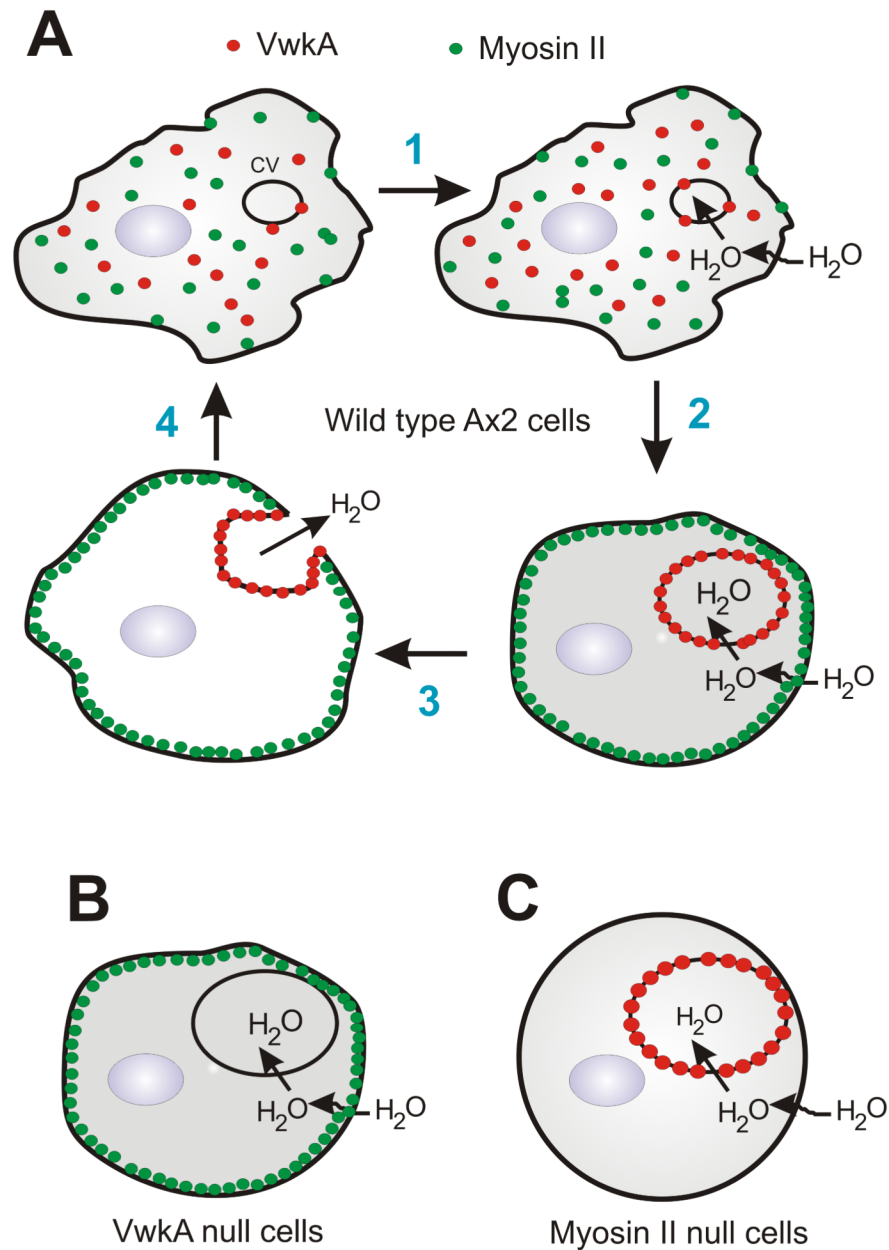


Figure 9. A model for the role of myosin II and Vwka in protecting amoeba from flooding
A. In this model, water influx leads to contractile vacuole growth, accompanied by recruitment of Vwka to the CV membrane (steps 1 & 2). Myosin II in the cortical cytoskeleton helps create cortical tension that has a positive role in CV fusion/expulsion, but by analogy to myosin II roles in adrenal chromaffin cells (35), myosin II may also have barrier roles, inhibiting CV fusion with the plasma membrane. Vwka is proposed to act on myosin II, either directly or indirectly, to disassemble/dissolve this cortical barrier, allowing CV-plasma membrane fusion and emptying to occur (step 3). **B.** We propose that in *vwka* null cells there is a defect in CV/plasma membrane fusion due to failure of the cortical cytoskeletal barrier of the cell to disassemble. **C.** Impaired CV fusion/expulsion in myosin II nulls cells is proposed to be a consequence of reduced cytosolic pressure in the absence of normal cortical contractility.